



HAL
open science

Deformation of Discrete Surfaces

Yukiko Kenmochi, Atsushi Imiya

► **To cite this version:**

Yukiko Kenmochi, Atsushi Imiya. Deformation of Discrete Surfaces. A. Rosenfeld; F. Sloboda; R. Klette. *Advances in Digital and Computational Geometry*, pp.285-316, 1998, 9813083948. hal-03037695

HAL Id: hal-03037695

<https://hal.science/hal-03037695>

Submitted on 11 Jan 2023

HAL is a multi-disciplinary open access archive for the deposit and dissemination of scientific research documents, whether they are published or not. The documents may come from teaching and research institutions in France or abroad, or from public or private research centers.

L'archive ouverte pluridisciplinaire **HAL**, est destinée au dépôt et à la diffusion de documents scientifiques de niveau recherche, publiés ou non, émanant des établissements d'enseignement et de recherche français ou étrangers, des laboratoires publics ou privés.

Deformation of Discrete Surfaces

Yukiko Kenmochi and Atsushi Imiya

Department of Information and Computer Sciences,
Chiba University
1-33 Yayoi-cho, Inage-ku, Chiba 263, JAPAN

Abstract. The deformation of surfaces is defined as a transformation of the surfaces while preserving their topology. In order to preserve the topology of surfaces under transformation, we introduce a polyhedral representation of surfaces using combinatorial topology. Combinatorial topology provides a way of representing surfaces by sets of triangles, more generally by sets of polygons. In this paper, we assume that a finite set of lattice points is given, and polyhedral surfaces are generated such that all points of the given set are surrounded by the polyhedral surfaces. Since all vertices of our polyhedral surfaces are assumed to be lattice points, we call those surfaces discrete surfaces. The deformation of discrete surfaces is described as the displacement of triangles or polygons which are considered to be the elements of discrete surfaces.

1 Introduction

The term “deformation” is used as the transformation of n -dimensional objects to n -dimensional objects while preserving their topology. In a 3-dimensional space, n can be from 0 to 3. Here, we consider the case where $n = 2$ and focus on the deformation of 2-dimensional closed surfaces which are the boundaries of 3-dimensional objects. The deformation of closed surfaces has been studied for volume segmentation of 3-dimensional objects as well as the snake which is a deformable curve around a 2-dimensional polygonal figure in a 2-dimensional plane [1]. From the viewpoint of other applications, the deformation of object surfaces is also useful for describing the motion between a sequence of images of 3-dimensional objects, for instance myocardial motion.

By comparison with deformation, skeletonization, thinning and localization of the medial axis are described as the transformation of n -dimensional objects to m -dimensional objects for $m \leq n$ [2, 3, 4, 5]. Because these transformations only preserve the connectivity of the points and sometimes do not consider and preserve the dimensions of objects, m can be less than n . According to our definition, deformation must be a transformation preserving not only the connectivities but also the dimensions of the objects.

For studying the deformation of closed surfaces in a computational space, representations of 3-dimensional objects and their boundaries are necessary. Since a computational space, such as a lattice space, is discrete, 3-dimensional objects in such a discrete space are called discrete objects. Several methods for the representation of discrete objects have been proposed. First, Kong and Rosenfeld [2]

and Voss [6] devised a method for representing discrete objects using the graph theory approach. The points of an object and the relations between the neighboring points correspond to the nodes and edges of an object graph. A graph is related to the data structure of a discrete object in a computer's memory, so that the nodes and the edges of the graph correspond to pointers and addresses of the computer, respectively. This approach, however, does not take into account the topological and geometric properties of discrete objects. Second, Herman [7] and Udupa [8] proposed a method for representing discrete objects, which contains the topological properties of the objects. In their method, a discrete object is represented by a set of voxels, or unit cubes, the centroids of which are lattice points. In addition, the boundary of a discrete object is represented by a set of voxel faces, which separate the object from its surroundings. Therefore, the boundary of a discrete object is represented not by a set of voxels but by a set of pairs of voxels, because a voxel face is determined by two adjacent voxels. Third, in 3-dimensional computer graphics, the marching cube method [9] is well known for the construction of the surface of a discrete object. This method generates a set of triangles surrounding a discrete object in a lattice space, so that the vertices of the triangles are determined by the interpolation the values between the lattice points, assuming that each lattice point has a gray value. However, this method sometimes generates unexpected holes in the surfaces of discrete objects. Lastly, Françon constructed discrete combinatorial surfaces [10] as 2-dimensional manifolds in a lattice space. He applied classical combinatorial topology in 3-dimensional Euclidean space to the definition of combinatorial manifolds in a lattice space.

Our method of representing discrete objects is similar to Françon's method and we also apply classical combinatorial topology [11]. In combinatorial topology, simplexes are fundamental for the description of the geometric properties of objects. Simplexes have the dimensions which can be from 0 to 3 in a 3-dimensional space. Simplexes of each dimension must be regarded as unit elements of the dimension. In 3-dimensional Euclidean space, 0-, 1-, 2-, and 3-dimensional simplexes are defined as isolated points, line segments, triangles and tetrahedra, respectively. Then, 3-dimensional objects are described by sets of 3-dimensional simplexes, and the boundary of an object which is a closed surface is described by a set of 2-dimensional simplexes. This representation is called a simplicial representation because it is defined as a combination of simplexes. In combinatorial topology [11], as an extension of the simplicial representation, a polyhedral representation is also presented. The polyhedral representation is considered if 2-dimensional surfaces are represented by general polygons instead of triangles and 3-dimensional objects are represented by general polyhedra instead of tetrahedra. Even if we employed the simplicial representation in references [12, 13], the polyhedral representation is used here because it yields an easy method for constructing closed surfaces in a 3-dimensional lattice space from a given set of lattice points.

This paper is arranged as follows. In section 2, we give an overview of the discrete combinatorial topology which is based on polyhedra. Since the discrete

combinatorial topology based on simplexes has been presented [12, 13], only simple modifications of the definitions are required, such as replacement of the term simplex by the term polyhedron. It is also shown that polyhedron-based combinatorial topology includes simplex-based combinatorial topology. In section 3, we present a polyhedral representation of 3-dimensional objects and the closed surfaces and compare it with the simplicial representation. A method for uniquely constructing polyhedral closed surfaces from a given set of a 3-dimensional lattice points is introduced in section 4, as well as the properties of constructed closed surfaces. This method requires two conversion steps: the first conversion is from a given finite set of lattice points to discrete objects and the second conversion is from discrete objects to the closed surfaces. In order to directly obtain the closed surfaces from a given set of lattice points, we present a practical algorithm in section 5. In section 6, we show that the polyhedral representation enables the classification of all points in 3-dimensional objects based on their local topological properties. The topological property of each point can be obtained from the local configuration of the neighboring points in the objects. These topological properties of the points enables us to employ the deformation of closed surfaces with preserving their 2-dimensional topological properties. In section 7, we then show a finite number of all the possible operations for the deformation as the displacement of a part of an the surface [14] and also an algorithm for the deformation between two different closed surfaces.

2 Discrete Combinatorial Topology

Let \mathbf{Z} be the set of all integers; \mathbf{Z}^3 is a set of lattice points which have only integer coordinates in a 3-dimensional Euclidean space \mathbf{R}^3 . It follows that \mathbf{Z}^3 is a subset of \mathbf{R}^3 . This section is devoted to presenting the fundamental properties of the combinatorial topology in \mathbf{Z}^3 . Classical combinatorial topology was built up for the representation and manipulation of n -dimensional objects in Euclidean spaces [11]. For example, 1-dimensional curves are represented by a set of connected line segments, 2-dimensional surfaces are represented by a set of connected polygons, such as triangles, and 3-dimensional objects are represented by a set of connected polyhedra, such as tetrahedra. If line segments and polygons are called 1- and 2-dimensional polyhedra respectively, we can say that an n -dimensional object is described by a set of n -dimensional polyhedra. These representations are then called polyhedral representations and the combinations of n -dimensional polyhedra are called n -dimensional polyhedral complexes in combinatorial topology. Among 2- and 3-dimensional polyhedra, triangles and tetrahedra are elementary polyhedra since their vertices are the minimum numbers required for 2- and 3-dimensional polyhedra; less than three or four vertices cannot constitute 2- or 3-dimensional polyhedra, respectively. Those elementary polyhedra are called n -dimensional simplexes and other n -dimensional polyhedra can be decomposed into n -dimensional simplexes. This decomposition is known as triangulation in combinatorial topology.

In \mathbf{Z}^3 , n -dimensional polyhedra are defined for $n = 0, 1, 2, 3$, so that the ver-

tices of those polyhedra are all lattice points. Those n -dimensional polyhedra in \mathbf{Z}^3 are called n -dimensional discrete polyhedra to distinguish them from the polyhedra in \mathbf{R}^3 . In this section, we first define a finite number of n -dimensional discrete polyhedra in a unit cubic region for $n = 0, 1, 2, 3$. These discrete polyhedra are called unit discrete polyhedra. From a set of unit discrete polyhedra, we choose elementary discrete polyhedra which cannot be decomposed into other discrete polyhedra. Then, we show that those elementary discrete polyhedra are equal to the discrete simplexes which are defined as simplexes in \mathbf{Z}^3 and referred to previously [12]. We also prove that any unit discrete polyhedron is always decomposed into several discrete simplexes. For the representation of 3-dimensional objects and the boundaries which are 2-dimensional surfaces in \mathbf{Z}^3 , we combine unit discrete polyhedra. The combinations of unit discrete polyhedra are referred to as polyhedral discrete complexes.

2.1 Unit Discrete Polyhedra

Let us consider all the possible convex polyhedra in a unit cube whose eight vertices are lattice points in \mathbf{Z}^3 so that the vertices of the convex polyhedra are also lattice points. To each vertex of the unit cube, we assign a binary value 1 or 0. Points with values 1 and 0 are called 1- and 0-points, respectively. Since there are eight vertices in a unit cube and each point can be either a 1- or 0-point, the number of all possible patterns of 1- and 0-points in a unit cube is 256. By considering rotational symmetry, these patterns can be reduced to 23. These are illustrated in Fig. 1. For each of the 23 patterns, we create a convex polyhedron such that the vertices of the convex polyhedron are 1-points. Let $\mathbf{x}_1, \mathbf{x}_2, \dots, \mathbf{x}_k$ be k lattice points. The closed convex hull of the k points is given by

$$CH(\{\mathbf{x}_1, \mathbf{x}_2, \dots, \mathbf{x}_k\}) = \{\mathbf{x} \in \mathbf{R}^3 \mid \mathbf{x} = \sum_{i=1}^k \lambda_i \mathbf{x}_i, \sum_{i=1}^k \lambda_i = 1, \lambda_i \geq 0\}.$$

Using the convex hull, we define unit discrete polyhedra.

Definition 1 Let $\mathbf{x}_1, \mathbf{x}_2, \dots, \mathbf{x}_k$ be 1-points in a unit cube of \mathbf{Z}^3 . If $CH(\{\mathbf{x}_1, \mathbf{x}_2, \dots, \mathbf{x}_k\})$ is an n -dimensional closed polyhedron, such as an isolated point, line segment, polygon or polyhedron for $n = 0, 1, 2, 3$, an n -dimensional unit discrete polyhedron is defined as

$$[\mathbf{x}_1, \mathbf{x}_2, \dots, \mathbf{x}_k] = \{\mathbf{x}_1, \mathbf{x}_2, \dots, \mathbf{x}_k\}.$$

Hereafter, we use the abbreviation of n -polyhedra for n -dimensional unit discrete polyhedra. Since polyhedra are bounded by polygons, polygons are bounded by line segments and line segments have endpoints, we can define the following set function.

Definition 2 Let $[a]$ be an n -polyhedron and $[b]$ be an s -polyhedron for $s < n$. If $CH([b])$ is included in the boundary of $CH([a])$, we say that $[b]$ is an s -face of $[a]$. The face of $[a]$ is defined as the set of all s -faces of $[a]$ for all $s < n$ and denoted by $face([a])$.

The following facts are easily derived from Definition 2: a 1-polyhedron includes two 0-faces, a 2-polyhedron includes 0- and 1-faces, and a 3-polyhedron includes 0-, 1- and 2-faces. For example, a tetrahedral 3-polyhedron includes four 0-faces, six 1-faces and four 2-faces. In \mathbf{Z}^3 , three different neighborhood systems are defined as follows.

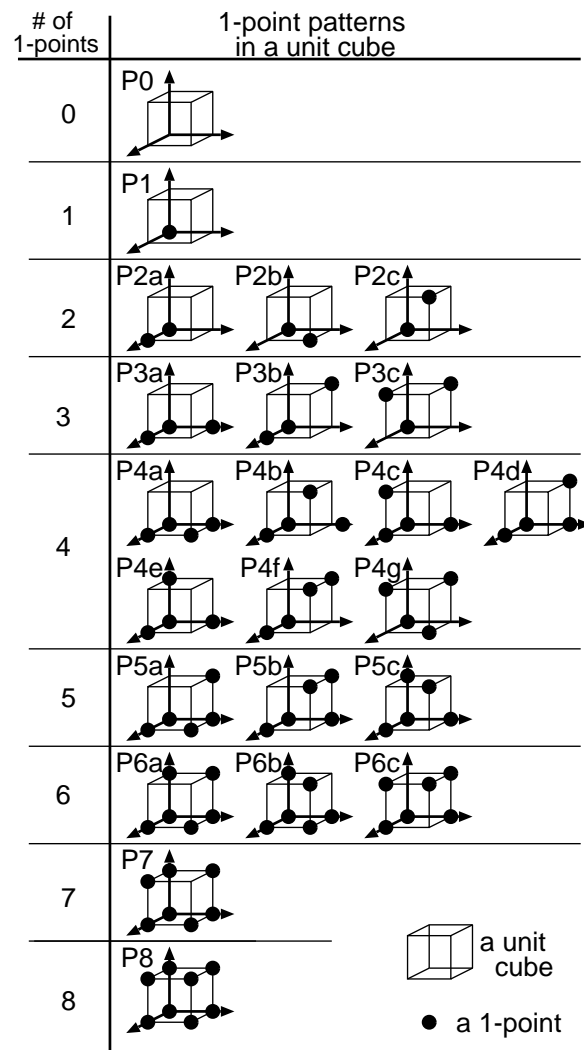


Fig. 1. Twenty-three possible patterns of 1- and 0-points in a unit cube; the set of all possible patterns is reduced by considering rotational symmetry in \mathbf{Z}^3 .

Definition 3 Let $\mathbf{x} = (i, j, k)$ be a point in \mathbf{Z}^3 . Three neighborhoods of \mathbf{x} are defined as

$$N_m(\mathbf{x}) = \{(p, q, r) \in \mathbf{Z}^3 \mid (i - p)^2 + (j - q)^2 + (k - r)^2 \leq t\},$$

for $m = 6, 18, 26$ corresponding to $t = 1, 2, 3$. They are called 6-, 18- and 26-neighborhoods, respectively.

With respect to each neighborhood system, we can determine a set of n -polyhedra for each $n = 0, 1, 2, 3$ as shown in Fig. 2. An isolated point of pattern P1 in Fig. 1 is regarded as a 0-polyhedron for any neighborhood system. Since two lattice points of a 1-polyhedron must be neighboring each other, a pair of points in pattern P2a are regarded as 1-polyhedron for any neighborhood system. A pair of points in pattern P2b, however, are not considered to be a 1-polyhedron for the 6-neighborhood system. Similarly, a pair of points in pattern P2c are considered to be a 1-polyhedron only for the 26-neighborhood system. Figure 2 illustrates that there are one, two and three 1-polyhedra for the 6-, 18- and 26-neighborhood systems, respectively. A 2-polyhedron is bounded by more than two 1-polyhedra which are the 1-faces of the 2-polyhedron. Therefore, it is concluded that there is only one 2-polyhedron of pattern P4a for the 6-neighborhood system. For the 18- and 26-neighborhood systems, there are four and five 2-polyhedra respectively. In a similar way, a 3-polyhedron is bounded by more than three 2-polyhedra which are the 2-faces of the 3-polyhedron. The determined 3-polyhedra for each neighborhood system are illustrated in the last line of Fig. 2.

Obviously, an n -polyhedron $[a]$ is a set of lattice points in \mathbf{Z}^3 and $CH([a])$ is the closed convex hull of $[a]$ which is defined in \mathbf{R}^3 . Thus, $CH([a])$ can be regarded as a convex polyhedron which is obtained by embedding $[a]$ into \mathbf{R}^3 . We define the embedded polyhedra of $[a]$ by a set of all interior points of $CH([a])$ as follows.

Definition 4 The embedded discrete polyhedron of an n -polyhedron $[a]$ is defined as

$$|a| = CH([a]) \setminus \left(\bigcup_{[b] \in \text{face}([a])} CH([b]) \right).$$

Clearly, $|a|$ is an open convex set in \mathbf{R}^3 . Using the embedded discrete polyhedra, we consider the decomposition of unit discrete polyhedra as follows. Let $[a]$ be an n -polyhedron. If

$$CH([a]) = \bigcup_{i=1}^k CH([b_i])$$

where $[b_i]$ is an n -polyhedron for $i = 1, 2, \dots, k$ and $[b_i] \cap [b_j] = \emptyset$ if $i \neq j$, then we say that $[a]$ can be decomposed into $[b_i]$ for $i = 1, 2, \dots, k$. If $[a]$ cannot be decomposed into more than one n -polyhedron, such $[a]$ is called an elementary n -polyhedron. The elementary n -polyhedra for $n = 0, 1, 2, 3$ with respect to each neighborhood system are shown as n -polyhedra with asterisks in Fig. 2. Figure

2 also shows that the set of all elementary n -polyhedra is equal to the set of n -dimensional discrete simplexes or n -simplexes which are already defined in reference [12]. The following theorem is then derived from Fig. 2.

Theorem 1 Any n -polyhedron of an m -neighborhood system can be decomposed into n -simplexes of the m -neighborhood system where $n = 0, 1, 2, 3$ for each $m = 6, 18, 26$.

dim.	unit discrete polyhedron		
	N ₆	N ₁₈	N ₂₆
0	*P1	*P1	*P1
1	*P2a	*P2a *P2b	*P2a *P2b *P2c
2	*P4a	*P3a *P3c P4a *P4f	*P3a *P3b *P3c P4a P4f
3	*P8	*P4e *P4g *P5b P5c P6a P6b P6c P7 P8	*P4b *P4c *P4d *P4e *P4g P5a P5b P5c P6a P6b P6c P7 P8

Fig. 2. Unit discrete polyhedra of dimensions from 0 to 3 for each of the 6-, 18- and 26-neighborhood systems. Note that n -polyhedra with asterisks are regarded as elementary n -polyhedra or n -simplexes for $n = 0, 1, 2, 3$.

2.2 Polyhedral Discrete Complex

In order to represent n -dimensional objects in \mathbf{Z}^3 , such as 1-dimensional curves, 2-dimensional surfaces and 3-dimensional objects, we combine unit discrete polyhedra as follows.

Definition 5 A finite set \mathbf{K} of unit discrete polyhedra is called a polyhedral discrete complex, if the following conditions are satisfied:

1. if $[a] \in \mathbf{K}$, $face([a]) \subseteq \mathbf{K}$;
2. if $[a_1], [a_2] \in \mathbf{K}$ and $|a_1| \cap |a_2| \neq \emptyset$, $[a_1] = [a_2]$,

where $[a]$ and $|a|$ are a unit discrete polyhedron and the corresponding embedded polyhedron, respectively.

The dimension of a polyhedral discrete complex \mathbf{K} is equal to the maximum dimension of all the unit discrete polyhedra which belong to \mathbf{K} . Hereafter, we abbreviate n -dimensional polyhedral discrete complexes to n -complexes as well as n -polyhedra. An n -complex is a combination of discrete polyhedra the dimensions of which are n and less than n . Two examples of 3-complexes for the 26-neighborhood system are illustrated in Fig. 3. Because of the second condition of Definition 5, two arbitrary unit discrete polyhedra included in a polyhedral discrete complex do not have any common points except for the points on their faces. In other words, discrete polyhedra do not intersect except at the lattice points. We introduce two properties of polyhedral discrete complexes, namely, purity and connectivity.

Definition 6 Let \mathbf{K} be an n -complex and $[a]$ be an s -polyhedron in \mathbf{K} where $s < n$. If every $[a]$ in \mathbf{K} satisfies the relation

$$[a] \in face([b])$$

where $[b]$ is an n -polyhedron in \mathbf{K} , \mathbf{K} is pure.

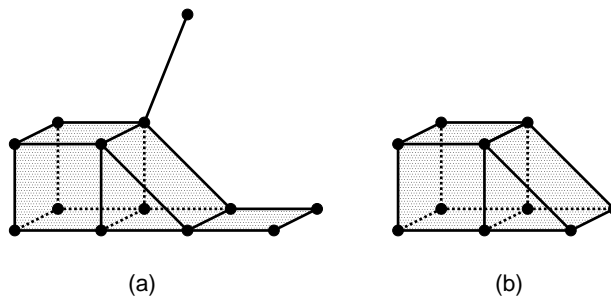


Fig. 3. Two examples of 3-complexes for the 26-neighborhood system: (a) a nonpure 3-complex and (b) a pure 3-complex. Both are connected.

Definition 7 Let \mathbf{K} be an n -complex. If we can define a path between two arbitrary elements $[a]$ and $[b]$ in \mathbf{K} , such as

$$[a_1] = [a], [a_2], \dots, [a_k] = [b],$$

where $[a_i] \in \mathbf{K}$ and $[a_i] \cap [a_{i+1}] \neq \emptyset$ for $i = 1, 2, \dots, k - 1$, \mathbf{K} is connected.

In a pure n -complex, unit discrete polyhedra of dimensions less than n do not exist unless they belong to the faces of the n -polyhedra. The 3-complex which is described by Fig. 3 (a) is not pure because it includes 1- and 2-polyhedra which do not belong to any 3-polyhedron. If we delete these 1- and 2-polyhedra from the nonpure 3-complex, the pure 3-complex which is illustrated by Fig. 3 (b) is obtained. Because the definition of polyhedral discrete complexes is not related to the connectivity, a polyhedral discrete complex can consist of several components of connected polyhedral discrete complexes. Each 3-complex in Fig. 3 is a connected 3-complex.

2.3 Simplicial Discrete Complex

If we replace the unit discrete polyhedra by discrete simplexes in Definition 5, we can define simplicial discrete complexes which consist of n -simplexes. Purity and connectivity can be also defined for simplicial discrete complexes. If we use n -simplexes for the representation of n -dimensional objects in \mathbf{Z}^3 instead of n -polyhedra, such a representation is called a simplicial representation. In this paper, however, we do not employ simplicial representations but use polyhedral representations. The reason for this is given in the next section.

3 Combinatorial Representation of Discrete Objects

3.1 Polyhedral Representation

The polyhedral representation of 3-dimensional objects in \mathbf{Z}^3 is given as follows.

Definition 8 Any pure and connected 3-complex is called a discrete object.

From a discrete object, we can obtain the boundary.

Definition 9 Let \mathbf{P} be a discrete object and \mathbf{H} be a set of 2-polyhedra in \mathbf{P} which belong to exactly one 3-polyhedron in \mathbf{P} . The boundary of \mathbf{P} is defined as

$$\partial\mathbf{P} = \mathbf{H} \cup \left(\bigcup_{[a] \in \mathbf{H}} \text{face}([a]) \right).$$

According to the definition, it is obvious that the boundary of a discrete object is a pure 2-complex. However, a pure 2-complex can be either connected or nonconnected; if a discrete object has a cavity inside it, the boundary consists of two components of connected and pure 2-complexes, one of which indicates the boundary of the cavity. Thus, we can say that the boundary of a discrete object consists of a finite number of connected and pure 2-complexes.

In addition to discrete objects, we define 2-dimensional surfaces in \mathbf{Z}^3 which we call discrete surfaces.

Definition 10 *Any pure and connected 2-complex is called a discrete surface.*

This definition enables us to say that the boundary of a discrete object consists of a finite number of discrete surfaces. The following theorem is then derived.

Theorem 2 *The boundary of a discrete object is a finite number of discrete closed surfaces, which are defined as discrete surfaces such that every 1-polyhedron included in the discrete surfaces belongs to more than one 2-polyhedron as the common face.*

Proof. According to Definition 8, a discrete object is generated by connecting 3-polyhedra together. Since every 3-polyhedron is completely bounded by a set of 2-polyhedra with no tear, a discrete object does not include any tear in the boundary. This is equivalent to the fact that every 1-polyhedron in the boundary belongs to more than one 2-polyhedron in the boundary.

3.2 Simplicial Representation

If we replace the term polyhedra by the term simplexes in all the definitions presented in the previous subsection, we obtain the simplicial representation of discrete objects and the surfaces. In references [12, 13], simplicial representations are used for discrete curves, surfaces and objects. The simplicial representation is a strong representation theoretically, and it is, however, too strong to apply to practical problems. One of our practical problems is to obtain a simplicial representation from a given set of lattice points. In order to solve this problem, the set of lattice points must be decomposed into 3-simplexes. This decomposition process is called triangulation in combinatorial topology. The triangulation, however, sometimes cannot be achieved or achieved uniquely as in the following cases:

- for the 26-neighborhood system, the triangulation cannot be determined uniquely even if it is achieved for any given set of lattice points. Figure 4 illustrates two different triangulations for a given set of lattice points;
- for the 18-neighborhood system, there is no guarantee of triangulation of a given set of lattice points. Figure 5 illustrates two examples of triangulation processes for given sets of lattice points. In case (a) the given set is triangulated and in case (b) the given set is not triangulated.

In order to avoid the above problems, a polyhedral representation of discrete objects and the surfaces are used in this paper.

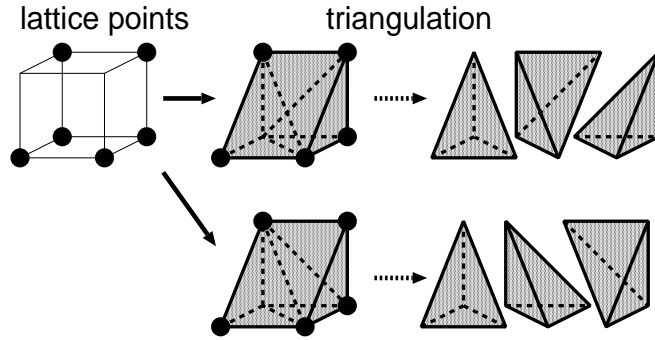


Fig. 4. An example of two different triangulations for a given set of lattice points. In this figure, the 26-neighborhood system is considered.

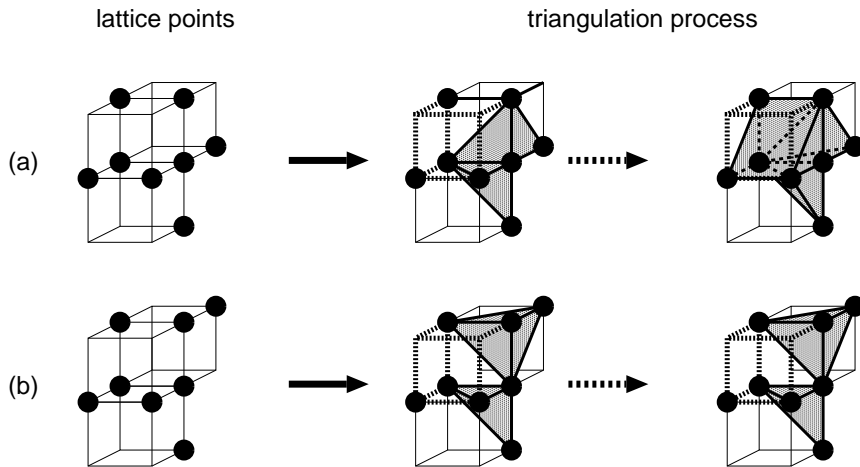


Fig. 5. Two example of triangulation processes for given sets of lattice points: triangulation is achieved in case (a) and triangulation is not completed in case (b). Both (a) and (b) are considered for the case of the 18-neighborhood system.

4 Construction of Discrete Object Surfaces

In this section, we assume that a finite subset \mathbf{V} of \mathbf{Z}^3 is given. It is also assumed that all the points in \mathbf{V} are 1-points and all the points in the complement of \mathbf{V} are 0-points. First, we decompose \mathbf{V} into a set of 3-polyhedra and then combine these 3-polyhedra to construct a pure 3-complex. Second, we separate the pure 3-complex by connectivity and obtain k polyhedral discrete objects \mathbf{P}_i for $i = 1, 2, \dots, k$. Finally, we extract the boundary $\partial\mathbf{P}_i$ from \mathbf{P}_i for each $i = 1, 2, \dots, k$.

4.1 First Stage: Polyhedral Decomposition of Lattice Points

In this stage, we construct a union of \mathbf{P}_i for $i = 1, 2, \dots, k$ from \mathbf{V} . This stage is mainly separated into two further steps. In the first step, we consider a 3-polyhedron for each unit cubic region in \mathbf{Z}^3 . The unit cube at a lattice point \mathbf{x} is defined by

$$D(\mathbf{x}) = N_{26}(\mathbf{x}) \cap N_{26}(\mathbf{y})$$

where $\mathbf{y} = (a + 1, b + 1, c + 1)$ if $\mathbf{x} = (a, b, c)$. Each $D(\mathbf{x})$ consists of eight lattice points which are the vertices of the unit cube. Each point of $D(\mathbf{x})$ is either a 1- or 0-point. The number of possible 1- and 0-point patterns of $D(\mathbf{x})$ is 23 as shown in Fig. 1, if we do not consider the patterns congruent with those in Fig. 1 by rotation symmetry. Among those 23 patterns in Fig. 1, there are some patterns for which we can determine the 3-polyhedra whereas for some patterns in Fig. 1 3-polyhedra cannot be constructed. The last line of Fig. 2 gives all the patterns for which we can determine the 3-polyhedra except pattern P5a for the 18-neighborhood system. Figure 6 illustrates an additional pattern P5a and the construction of a 3-polyhedron in the case of the 18-neighborhood system. Note that we cannot determine any 3-polyhedra for the other patterns which are not given in the last line of Fig. 2 and by Fig. 6.

In the second step, we combine the 3-polyhedra at all $D(\mathbf{x})$ in \mathbf{Z}^3 and construct k discrete objects \mathbf{P}_i for all $i = 1, 2, \dots, k$. Let $[a]$ and $[b]$ be two 3-polyhedra in adjacent unit cubes. The possible relationships between $[a]$ and $[b]$ with regard to their adjacency are classified into the following five cases:

1. $[a]$ and $[b]$ share a 0-face in common as shown in Fig. 7 (a);
2. $[a]$ and $[b]$ share a 1-face in common as shown in Fig. 7 (b);
3. $[a]$ and $[b]$ share a 2-face in common as shown in Fig. 7 (c);
4. a 2-face of $[b]$ is included in a 2-face of $[a]$ as shown in Fig. 7 (d);
5. a 2-face of $[a]$ and a 2-face of $[b]$ have a common 1-face but neither an equality nor an inclusion relation holds between them as shown in Fig. 7 (e).

The fourth case appears only if the neighboring system is the 18-neighborhood one and $[b]$ is obtained from pattern P5a in Fig. 6. Similarly, the fifth case also appears only if the neighboring system is the 18-neighborhood one and in addition, both $[a]$ and $[b]$ are obtained from pattern P5a as illustrated in Fig. 7 (e). Figure 7 indicates that the combination of $[a]$ and $[b]$ can constitute a 3-complex \mathbf{P} such as

$$\mathbf{P} = \{[a], [b]\} \cup \text{face}([a]) \cup \text{face}([b]) \quad (1)$$

if their adjacent relation is either (a), (b) or (c) in Fig. 7. Since only the three relations (a), (b) and (c) appear for the 6- and 26-neighborhood systems, the following conclusion is derived. Let $[a(\mathbf{x})]$ be a 3-polyhedron in $D(\mathbf{x})$. Then, a union of discrete objects \mathbf{P}_i for $i = 1, 2, \dots, k$ is constructed such as

$$\bigcup_{i=1}^k \mathbf{P}_i = \bigcup_{\mathbf{x} \in \mathbf{Z}^3} (\{[a(\mathbf{x})]\} \cup \text{face}([a(\mathbf{x})])) \quad (2)$$

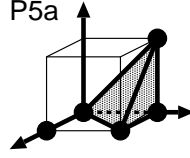


Fig. 6. An additional pattern P5a for which we can determine a 3-polyhedron in the case of the 18-neighborhood system. All the other patterns are given in the last line of Fig. 2.

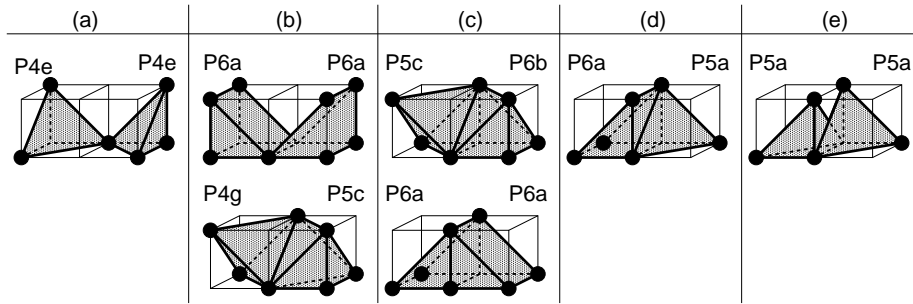


Fig. 7. The five different relations between two 3-polyhedra $[a]$ and $[b]$ in the adjacent unit cubes are shown by the following examples. (a) $[a]$ and $[b]$ share a 0-face in common, (b) $[a]$ and $[b]$ share a 1-face in common, (c) $[a]$ and $[b]$ share a 2-face in common, (d) a 2-face of $[b]$ is included in a 2-face of $[a]$ and (e) a 2-face of $[a]$ and a 2-face of $[b]$ have a common 1-face but there is neither an equality nor an inclusion relation between them. All the five cases are illustrated for the 18-neighborhood system. Note that cases (d) and (e) do not appear for the 6- and 26-neighborhood systems.

for the 6- and 26-neighborhood systems.

In order to construct discrete objects for the 18-neighborhood system, we have to consider additional processes before the process of combining 3-polyhedra which is described by (2) if the adjacent relation (d) or (e) in Fig. 7 appears. First, we present the method to avoid the adjacent relation (d). Let $[a]$ and $[b]$ be two 3-polyhedra whose adjacent relation is (d) in Fig. 7. If a 2-face $[c]$ of $[b]$ is included in a 2-face $[d]$ of $[a]$, then $[c]$ can be divided into two 2-polyhedra $[d]$ and $[e]$ such as

$$CH([c]) = CH([d]) \cup CH([e])$$

where $|d| \cap |e| = \emptyset$. This enables us to replace $[c]$ by $[d]$ and $[e]$ in $face([b])$. The replacement changes the adjacent relation between $[a]$ and $[b]$ from (d) to (c) in Fig. 7 and the combination of $[a]$ and $[b]$ constitutes a 3-complex \mathbf{P} as in (1). Second, we consider a method for avoiding the adjacent relation of (e) in Fig. 7. There is, however, no method except for ignoring the two 3-polyhedra which have the adjacent relation of (e) in Fig. 7. If we completely ignore them, we can construct discrete objects such as in equation (2). Note that the relation (e) in

Fig. 7 rarely appears because both $[a]$ and $[b]$ must be constructed in unit cubes with pattern P5a.

Thus, we can obtain $\cup_{i=1}^k \mathbf{P}_i$ from \mathbf{V} for any neighborhood system. The following theorem is then derived.

Theorem 3 *Let \mathbf{Q}_6 , \mathbf{Q}_{18} and \mathbf{Q}_{26} be the unions of discrete objects which are obtained from \mathbf{V} for the 6- 18- and 26-neighborhood systems, respectively. For any \mathbf{V} , the relation*

$$\bigcup_{[a_6] \in \mathbf{Q}_6} |a_6| \subseteq \bigcup_{[a_{18}] \in \mathbf{Q}_{18}} |a_{18}| \subseteq \bigcup_{[a_{26}] \in \mathbf{Q}_{26}} |a_{26}| \quad (3)$$

always holds.

Proof. Let $[a_m(\mathbf{x})]$ be a 3-polyhedron with respect to the m -neighborhood system in a unit cube $D(\mathbf{x})$ for $m = 6, 18, 26$. For any 1-point pattern of a unit cubic region, the relation

$$|a_6(\mathbf{x})| \subseteq |a_{18}(\mathbf{x})| \subseteq |a_{26}(\mathbf{x})|$$

holds as derived from Fig. 2 and Fig. 6. Since

$$\mathbf{Q}_m = \bigcup_{\mathbf{x} \in \mathbf{Z}^3} (\{[a_m(\mathbf{x})]\} \cup \text{face}([a_m(\mathbf{x})])),$$

the relation (3) is satisfied.

4.2 Second Stage: Object Separation by Connectivity

Since $\cup_{i=1}^k \mathbf{P}_i$ is a pure 3-complex and we do not consider the connectivity, it is necessary to decompose $\cup_{i=1}^k \mathbf{P}_i$ into each connected \mathbf{P}_i . Because the decomposition of a 2-complex into connected complexes will be necessary in the following section, we discuss the decomposition process by generalizing the dimensions of the decomposed complexes. Let \mathbf{C}_n be the set of all n -polyhedra in a pure n -complex. Then a connected set of n -polyhedra is selected from \mathbf{C}_n as follows:

Algorithm 1

input: *The set of n -polyhedra in a pure n -complex, \mathbf{C}_n .*

output: *Connected pure n -complexes, $\mathbf{X}_1, \mathbf{X}_2, \dots, \mathbf{X}_p$.*

begin

1. *Set $i := 0$;*

2. **while** $\mathbf{C}_n \neq \emptyset$ **do**

2.1 *set $i := i + 1$; $\mathbf{X}_i := \emptyset$;*

2.2 *select an element $[a]$ from \mathbf{C}_n and set $\mathbf{C}_n := \mathbf{C}_n \setminus [a]$; $\mathbf{X}_i := \mathbf{X}_i \cup [a]$;*

2.3 **while** $[b]$ exists in \mathbf{C}_n such that $[b] \cap [c] \neq \emptyset$ and $[c] \in \mathbf{X}_i$ **do**

set $\mathbf{C}_n := \mathbf{C}_n \setminus [b]$; $\mathbf{X}_i := \mathbf{X}_i \cup [b]$.

end

The counter i in the first **while** loop in Step 2 is equal to the number of connected sets in \mathbf{C}_n and the first **while** loop creates the connected set \mathbf{X}_i for each $i = 1, 2, \dots, p$. The second **while** loop in step 2.3 removes all n -polyhedra, which are connected to the elements of \mathbf{X}_i , from \mathbf{C}_n and adds them to \mathbf{X}_i . If we apply this algorithm to $\cup_{i=1}^k \mathbf{P}_i$, \mathbf{P}_i for every $i = 1, 2, \dots, k$ is obtained.

4.3 Third Stage: Surface Extraction from Discrete Objects

According to Definition 9, if we can obtain set \mathbf{H} in Definition 9 from \mathbf{P}_i , $\partial\mathbf{P}_i$ is derived from \mathbf{H} for each $i = 1, 2, \dots, k$. Let \mathbf{C}_3 be the entire set of 3-polyhedra in \mathbf{P}_i and \mathbf{C}_2 be the entire set of 2-polyhedra in \mathbf{P}_i . Then, set \mathbf{H} in Definition 9 is obtained from \mathbf{C}_2 by checking for each 2-polyhedron in \mathbf{C}_2 how many 3-polyhedra in \mathbf{C}_3 include the 2-polyhedron. If the 2-polyhedron is included in two 3-polyhedra in \mathbf{C}_3 , the 2-polyhedron is located inside \mathbf{P}_i and does not belong to \mathbf{H} . If the 2-polyhedron is included in exactly one 3-polyhedron in \mathbf{C}_3 , the 2-polyhedron is on the boundary of \mathbf{P}_i and belongs to \mathbf{H} .

The following theorem is derived from all the processes for the construction of $\partial\mathbf{P}_i$ for $i = 1, 2, \dots, k$ from \mathbf{V} via \mathbf{P}_i .

Theorem 4 *For each neighborhood, $\partial\mathbf{P}_i$ for $i = 1, 2, \dots, k$ are uniquely obtained from \mathbf{V} .*

Proof. There are three conversion steps from \mathbf{V} to $\partial\mathbf{P}_i$ for $i = 1, 2, \dots, k$: the first step is the conversion from \mathbf{V} to $\cup_{i=1}^k \mathbf{P}_i$; the second step is the conversion from $\cup_{i=1}^k \mathbf{P}_i$ to \mathbf{P}_i for $i = 1, 2, \dots, k$; the third step is the conversion from \mathbf{P}_i to $\partial\mathbf{P}_i$ for each $i = 1, 2, \dots, k$. In each step, the conversion is uniquely done. For instance, $\cup_{i=1}^k \mathbf{P}_i$ is uniquely obtained from \mathbf{V} since a 3-polyhedron at each unit cube is uniquely obtained and all 3-polyhedra in \mathbf{V} are also uniquely combined. Thus, it is said that $\partial\mathbf{P}_i$ for $i = 1, 2, \dots, k$ are uniquely obtained from \mathbf{V} for each neighborhood.

5 Algorithm of Discrete Closed Surface Construction

According to the previous section, $\partial\mathbf{P}_i$ for $i = 1, 2, \dots, k$ are uniquely obtained from \mathbf{V} via \mathbf{P}_i . For practical applications, there is an algorithm of directly obtaining $\partial\mathbf{P}_i$ for $i = 1, 2, \dots, k$ from \mathbf{V} using Table 1 for each neighborhood system. The table is created by ignoring the 3-polyhedral structures inside \mathbf{P}_i and extracting only 2-polyhedra on the boundary of \mathbf{P}_i , since we need only $\partial\mathbf{P}_i$ and not the inside of \mathbf{P}_i . The reason why the term ‘‘candidate’’ is used in Table 1 is that some of the 2-polyhedra in Table 1 may not constitute $\partial\mathbf{P}_i$; further explanations will be given later. The arrows shown in Table 1 point to the outside of \mathbf{P}_i .

From Theorem 2, $\partial\mathbf{P}_i$ for each $i = 1, 2, \dots, k$ consists of a finite number of discrete closed surfaces. Let \mathbf{S}_i for $i = 1, 2, \dots, p$ be p discrete closed surfaces which are included in a union of $\partial\mathbf{P}_i$ for $i = 1, 2, \dots, k$. Then, \mathbf{S}_i for $i = 1, 2, \dots, p$ are obtained directly from \mathbf{V} by the following algorithm.

Algorithm 2

input: A set of lattice points, \mathbf{V} , whose z -axis range is from 0 to l .

output: Discrete closed surfaces $\mathbf{S}_1, \mathbf{S}_2, \dots, \mathbf{S}_p$.

begin

1. Set the discrete-closed-surface number $i := 0$.

2. **For** $0 \leq j \leq l$ **do**

2.1 **If** $j \neq l$ **then**

2.1.1 Let T_j be the set of candidates of 2-polyhedra, which are looked up for each unit cube between two planes $z = j$ and $z = j + 1$ in Table 1 for each neighborhood system.

2.1.2 **If** T_j includes a pair of candidates whose vertices are all the same, **then** delete the pair from T_j .

2.2 **If** $j \neq 0$, **then**

2.2.1 **If** T_{j-1} and T_j have common candidates such that their vertices are all the same, **then** delete those candidates from both T_{j-1} and T_j .

2.2.2 Decompose T_{j-1} into TT_1, TT_2, \dots, TT_q , using connectivity as in Algorithm 1.

2.2.3 **For** $1 \leq u \leq q$ **do**

If points in TT_u are included in several \mathbf{S}_r s where $0 < r < i + 1$, **then** let \mathbf{S}_r be the union of these \mathbf{S}_r s and TT_u , where r' is the smallest r , and the other \mathbf{S}_r s be empty sets, **else**, set $i := i + 1$; $\mathbf{S}_i := TT_u$.

3. Reenumerate the sets of discrete closed surfaces, skipping empty sets.

end

Our algorithm is a slice by slice algorithm and requires the scanning of every slice once to construct all \mathbf{S}_i for $i = 1, 2, \dots, p$. If the size of an xy -plane slice of \mathbf{V} is $M \times N$ and the maximum memory space for storing all the 2-polyhedral candidates in a unit cube is K , then we need at most $K \times M \times N \times 2$ memory space for storing all 2-polyhedral candidates in two adjacent slices. For the i th slice, the algorithm is separated into four procedures: look up 2-polyhedral candidates in the table for every unit cube in the slice in step 2.1.1; delete any extra candidates which do not constitute discrete closed surfaces from the set of candidates in steps 2.1.2 and 2.2.1; decompose the set of candidates into connected subsets in step 2.2.2; assign each of these connected subsets to \mathbf{S}_i in step 2.2.3.

In the first procedure of step 2.1.1, we precalculate the vertices of the 2-polyhedral candidates for every index which corresponds to a pattern of 1- and 0-points in a unit cube. The index can be from 0 to 255 since each of eight vertices of a unit cube is either a 1- or 0-point and there are 256 possible patterns of 1- and 0-points in a unit cube. For instance, the index is 0 if all the points in a unit cube are 0-points, and is 255 if all the points are 1-points. Every unit cube in \mathbf{Z}^3 has an index and the 2-polyhedral candidates in each unit cube are obtained using the index. Note that there is no 2-polyhedral candidate for unit cubes with the indexes 0 and 255 according to Table 1. The unit cubes with index 0 or 255

# of 1-points	candidates of 2-polyhedra for discrete object surfaces		
	N ₆	N ₁₈	N ₂₆
3		P3a 	
4	P4a 	<div style="display: flex; flex-wrap: wrap;"> <div style="width: 50%; text-align: center;">P4a </div> <div style="width: 50%; text-align: center;">P4b </div> <div style="width: 50%; text-align: center;">P4c </div> <div style="width: 50%; text-align: center;">P4d </div> <div style="width: 50%; text-align: center;">P4e </div> <div style="width: 50%; text-align: center;">P4g </div> </div>	<div style="display: flex; flex-wrap: wrap;"> <div style="width: 50%; text-align: center;">P4a </div> <div style="width: 50%; text-align: center;">P4b </div> <div style="width: 50%; text-align: center;">P4c </div> <div style="width: 50%; text-align: center;">P4d </div> <div style="width: 50%; text-align: center;">P4e </div> <div style="width: 50%; text-align: center;">P4g </div> </div>
5	P5a 	<div style="display: flex; flex-wrap: wrap;"> <div style="width: 50%; text-align: center;">P5a </div> <div style="width: 50%; text-align: center;">P5b </div> <div style="width: 50%; text-align: center;">P5c </div> </div>	<div style="display: flex; flex-wrap: wrap;"> <div style="width: 50%; text-align: center;">P5a </div> <div style="width: 50%; text-align: center;">P5b </div> <div style="width: 50%; text-align: center;">P5c </div> </div>
6	<div style="display: flex; flex-wrap: wrap;"> <div style="width: 50%; text-align: center;">P6a </div> <div style="width: 50%; text-align: center;">P6b </div> </div>	<div style="display: flex; flex-wrap: wrap;"> <div style="width: 33%; text-align: center;">P6a </div> <div style="width: 33%; text-align: center;">P6b </div> <div style="width: 33%; text-align: center;">P6c </div> </div>	
7	P7 	P7 	

Table 1. The look-up table which provides the one-to-one correspondence between a pattern of 1-points in a unit cube and the 2-polyhedra candidates for discrete closed surfaces with respect to each neighborhood system.

are located on the inside or outside of the discrete objects, respectively, since the eight points in a unit cube for index 0 or 255 are all assigned 0- or 1-points. A similar method using indexes is also employed in the marching cubes method [9].

In the second procedure of steps 2.1.2 and 2.2.1, we consider the case in which two adjacent unit cubes have a common candidate as shown in Fig. 8. Note that the common candidate has two oppositely directed arrows, each of which points to the inside of each of the unit cubes. If such candidates are extracted from \mathbf{V}

with reference to Table 1, we have to delete them because they do not form a part of the discrete closed surfaces. In steps 2.1.2 and 2.2.1, we search for the common candidate of two adjacent unit cubes; in step 2.1.2 the two adjacent unit cubes are both in an i th slice, and in step 2.2.1 each of the two adjacent unit cubes are in either of the two adjacent slices. This deleting procedure is employed if \mathbf{V} includes 2-dimensional parts as shown in Fig. 3 (a) at the joint of two adjacent unit cubes. Otherwise, the procedure achieves nothing.

For the 18-neighborhood system, there is a case where we have to ignore two adjacent 3-polyhedra which are shown in Fig. 7 (e). Since 2-faces of these two 3-polyhedra should be included in a part of \mathbf{S}_i , we have to replace the 2-polyhedral candidates at two adjacent unit cubes whose 1-point patterns are both P5a as described by Fig. 9. The following additional step is inserted in step 2.1.2 (resp. 2.2.1) of Algorithm 2 for the 18-neighborhood system.

- If the 18-neighborhood system is considered, check whether T_j (resp. a union of T_{j-1} and T_j) includes sets of four 2-polyhedra which are illustrated in the left side of Fig. 9. If so, exclude those 2-polyhedra from T_j (resp. a union of T_{j-1} and T_j) and add pairs of 2-polyhedra which are illustrated in the right side of Fig. 9 to T_j (resp. a union of T_{j-1} and T_j) instead.

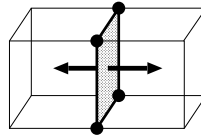


Fig. 8. An example of a case in which two adjacent unit cubes have a common 2-polyhedral candidate. If such 2-polyhedral candidates are extracted from \mathbf{V} , they are ignored for the construction of discrete closed surfaces.

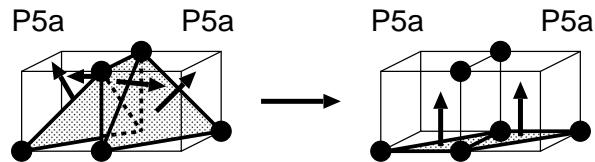


Fig. 9. Replacement of 2-polyhedral candidates at two adjacent unit cubes of the patterns P5a. This replacement enables us to construct discrete closed surfaces without contradiction. Note that this replacement is employed in the 18-neighborhood system only.

6 Topology of Points

Using the following two set functions, which are a star and the outer boundary of a star [11, 12], we classify all the points in discrete objects.

Definition 11 *Let \mathbf{K} be a discrete object (discrete closed surface) and \mathbf{x} be a point in \mathbf{K} ; the star of \mathbf{x} with respect to \mathbf{K} is defined as*

$$\sigma(\mathbf{x} : \mathbf{K}) = \{[a] \in \mathbf{K} \mid \mathbf{x} \in [a]\}.$$

Definition 12 *Let \mathbf{K} be a discrete object (discrete closed surface) and \mathbf{x} be a point in \mathbf{K} ; the outer boundary of $\sigma(\mathbf{x} : \mathbf{K})$ is defined as*

$$[\sigma(\mathbf{x} : \mathbf{K})] = \left(\bigcup_{[a] \in \sigma(\mathbf{x} : \mathbf{K})} \text{face}([a]) \right) \setminus \sigma(\mathbf{x} : \mathbf{K}).$$

We define two topological types for points of a discrete object as follows.

Definition 13 *Let \mathbf{P} be a discrete object and \mathbf{x} be a point in \mathbf{P} . If $[\sigma(\mathbf{x} : \mathbf{P})]$ constitutes a discrete closed surface, then \mathbf{x} is spherical.*

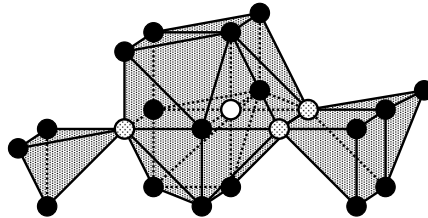
Definition 14 *Let \mathbf{P} be a discrete object and \mathbf{x} be a point in \mathbf{P} . If $[\sigma(\mathbf{x} : \mathbf{P})]$ constitutes a discrete surface which is not closed, then \mathbf{x} is semi-spherical.*

These two topological types of points are depicted in Fig. 10. Spherical points indicate the interior points of discrete objects and semi-spherical points indicate points on the boundaries of discrete objects, except for the intersections of the boundaries. Because points which are the intersections of the boundaries are regarded as neither spherical nor semi-spherical, we call these points singular points. Several examples of singular points are also illustrated in Fig. 10. It is obvious that every point on the boundary of a discrete object is either semi-spherical or singular, but not spherical. Using these topological properties of points, it is possible to distinguish points on the boundary of a discrete object from all points in a discrete object. In addition, it is also possible to extract intersections from points on the boundary.

If the boundary of a discrete object is given instead of the entire discrete object, however, we cannot distinguish between intersections and other points on the boundary which is a set of discrete closed surfaces. This is because we cannot calculate the above topological types of points from the boundary of a discrete object. In order to solve this problem, we define another topological type of point which we can determine from the boundary.

Definition 15 *Let \mathbf{S} be a discrete closed surface and \mathbf{x} be a point in \mathbf{S} . If $[\sigma(\mathbf{x} : \mathbf{S})]$ makes a circle, such as a path of connected 1-polyhedra which does not intersect and whose beginning and end points are the same, then \mathbf{x} is cyclic.*

Cyclic points are equivalent to semi-spherical points, as shown in Fig. 10. All points on a discrete closed surface, except for cyclic points, are called singular points of the discrete closed surface as well as singular points of a discrete object.



- a spherical point
- a semi-spherical (cyclic) point
- ⊗ a singular point

Fig. 10. Three topological types of points of discrete objects: spherical, semi-spherical (cyclic) and singular points which indicate interior, boundary and intersection points of a discrete object. The example shown is in the case of the 26-neighborhood system.

7 Deformation and Topology

Let \mathbf{P} be a discrete object and $\partial\mathbf{P}$ be the boundary of \mathbf{P} which is a set of finite numbers of discrete closed surfaces. Then a deformation of $\partial\mathbf{P}$ is defined as a process of expanding or shrinking $\partial\mathbf{P}$ while preserving its topology. In this paper, an Euler characteristic is considered to be a topological parameter of $\partial\mathbf{P}$. The Euler characteristic $E(\partial\mathbf{P})$ is given by

$$E(\partial\mathbf{P}) = \mathbf{V} - \mathbf{E} + \mathbf{F} ,$$

where \mathbf{V} , \mathbf{E} and \mathbf{F} are the numbers of the 0-, 1- and 2-polyhedra in $\partial\mathbf{P}$ [15]. Now, let \mathbf{P}' be a discrete object whose boundary $\partial\mathbf{P}'$ is a deformation of $\partial\mathbf{P}$. We see that the deformation preserves the topology if and only if

$$E(\partial\mathbf{P}) - E(\partial\mathbf{P}') = 0 \tag{4}$$

holds; in this case, not only the number of singular points but also their locations and their topological structures, such as the configuration of connected 2-polyhedra around the singular points, do not change between $\partial\mathbf{P}$ and $\partial\mathbf{P}'$.

7.1 Polyhedral Deformation

Deformation operations for $\partial\mathbf{P}$ are mainly classified into two classes: one consists of operations for expanding $\partial\mathbf{P}$ and the other consists of operations for shrinking $\partial\mathbf{P}$. We call them expanding and shrinking deformations, respectively. An expanding deformation is equivalent to a process of increasing the volume of \mathbf{P} while preserving its topology. In order to increase the volume of \mathbf{P} , we attach 3-polyhedra to $\partial\mathbf{P}$. By contrast, a shrinking deformation is described as

a process of decreasing the volume of \mathbf{P} while preserving its topology, so that we remove 3-polyhedra from $\partial\mathbf{P}$.

First, we focus on the operations of expanding deformations. Let $[a]$ be a 3-polyhedron attached to $\partial\mathbf{P}$; $face([a])$ is the boundary of $[a]$ and constitutes a discrete closed surface. We divide $face([a])$ into two nonempty discrete surfaces **Old** and **New** as follows:

$$\mathbf{Old} = face([a]) \cap \partial\mathbf{P} , \quad (5)$$

$$\mathbf{New} = \bigcup_{[b] \in (face([a]) \setminus \mathbf{Old})} (\{[b]\} \cup face([b])) . \quad (6)$$

Then, a discrete object \mathbf{P}' is determined so that

$$\partial\mathbf{P}' = (\partial\mathbf{P} \setminus \mathbf{Old}) \cup \mathbf{New} . \quad (7)$$

In such a case, we call $\partial\mathbf{P}'$ expanded discrete surfaces of $\partial\mathbf{P}$. When singular points are included in $\partial\mathbf{P}$, a deformation operation obtaining $\partial\mathbf{P}'$ from $\partial\mathbf{P}$ as above sometimes does not preserve the topology. In our discussion, we treat only deformations preserving topology; such deformations give no topological change on the set of singular points. In fact, we check that the following conditions are satisfied before and after our deformation operations:

- all points in **Old** are cyclic with respect to $\partial\mathbf{P}$;
- all points in **New** are cyclic with respect to $\partial\mathbf{P}'$.

Shrinking deformation is the inverse of expanding deformation. Let $[a]$ be the 3-polyhedron removed from $\partial\mathbf{P}$. Then, the shrunk discrete surfaces $\partial\mathbf{P}'$ of $\partial\mathbf{P}$ is derived from (7) as well as **Old** and **New** are from (5) and (6), respectively. But note that $[a]$ is located inside \mathbf{P} in the case of shrinking deformation.

7.2 Simplicial Deformation

In order to simplify the relation between the deformation of $\partial\mathbf{P}$ and the topology preservation, we expand (resp. shrink) $\partial\mathbf{P}$ by attaching (resp. removing) some 3-simplexes instead of a 3-polyhedron. From Theorem 1, the following theorem is easily derived.

Theorem 5 *Any deformation operation by a 3-polyhedron is a composition of several deformation operations by 3-simplexes.*

In this subsection, we consider the simplicial representation of $\partial\mathbf{P}$. In fact, based on Theorem 1, we obtain the simplicial representation of $\partial\mathbf{P}$ from the polyhedral one. Hereafter, a deformation by a 3-simplex is called a simplicial deformation while a deformation by a 3-polyhedron is called a polyhedral deformation.

A simplicial deformation of $\partial\mathbf{P}$ is given by (7) with **Old** and **New** obtained from (5) and (6), in the case when $[a]$ is a 3-simplex. We first consider simplicial deformation operations for expanding $\partial\mathbf{P}$. All possible pairs of **New** and **Old** in the expanding deformation process are illustrated in Fig. 11 for each 3-simplex

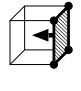



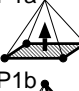










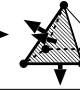

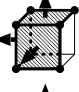



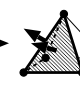

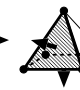
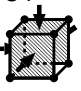
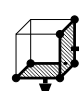

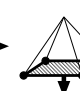


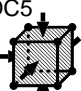
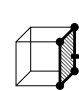
# of 2-faces in Old	(a) cubic 3-simplex		(b) tetrahedral 3-simplex		(c) pentahedral 3-simplex			
	Old	→ New	Old	→ New	Old	→ New		
1	DC1 		DT1 		DP1a 		DP1b 	
2	DC2 		DT2 		DP2a 		DP2b 	
3	DC3a 		DT3 		DP3a 		DP3b 	
4	DC4 				DP4a 		DP4b 	
5	DC5 							

Fig. 11. All possible deformation operations for expanding $\partial\mathbf{P}$ using a cubic 3-simplex in the 6-neighborhood system (a), using a tetrahedral 3-simplex in the 18- and 26-neighborhood systems (b), and using a pentahedral 3-simplex in the 18-neighborhood system (c). Note that $\partial\mathbf{P}$ is expanded to $(\partial\mathbf{P} \setminus \mathbf{Old}) \cup \mathbf{New}$. Deformation operations for shrinking are obtained if we replace **Old** by **New** and **New** by **Old** respectively for each operation in this figure.

shape in each neighborhood system. In the 6-neighborhood system, every 3-simplex forms a cube and has six square 2-faces, as shown in Fig. 2. Because each 2-face in a 3-simplex is included either in **Old** or in **New**, at most five 2-faces are included in **Old**. In each case of the numbers of 2-faces in **Old**, there is only one configuration of 2-faces in **Old** and **New**, except in the case of three 2-faces belonging to **Old**. In this case, there exist two different 2-face configurations DC3a and DC3b as shown in Fig. 11. In the 18-neighborhood system, 3-simplexes

are either tetrahedral or pentahedral. In the case of expanding deformation by a tetrahedral 3-simplex, there are three configurations of 2-faces in **Old** and **New**, while there are eight configurations in the case of expanding deformation by a pentahedral 3-simplex. Similarly, in the 26-neighborhood system, there are three configurations of 2-faces in **Old** and **New**, because all 3-simplexes are tetrahedral.

Shrinking deformation is the inverse of expanding one. Thus, by replacing **Old** by **New** and **New** by **Old** respectively in Fig. 11, we obtain the set of all deformation operations for shrinking since the set of all operations for expanding are shown in Fig. 11.

Because Fig. 11 describes only the process of expanding operation of $\partial\mathbf{P}$ by a 3-simplex, we must employ the operation n times if necessary, to expand (resp. shrink) $\partial\mathbf{P}$ as we like. Obviously, the result of a series of n expanding (resp. shrinking) operations depends on the choice of **Old** for each operation. The further discussion is done in subsection 7.5.

7.3 Elementary Deformation Operations

According to Theorem 5, a polyhedral deformation operation is a composition of simplicial deformation operations. In this subsection, we also prove that any simplicial deformation operation by a cubic or pentahedral 3-simplex in the 6- or 18-neighborhood system can be decomposed into a set of several operations by tetrahedral 3-simplexes in the 26-neighborhood system. We give two examples of the decomposition of an operation in Fig. 12. The first example shows that an operation for expanding deformation by a cubic 3-simplex is a composition of six operations by tetrahedral 3-simplexes. Similarly, the second example shows that an operation for expanding deformation by a pentahedral 3-simplex is a composition of two operations by tetrahedral 3-simplexes. Those are because any cubic or pentahedral 3-simplex can be always decomposed into several tetrahedral 3-simplexes in a way similar to the decomposition of 3-polyhedra by 3-simplexes. Consequently, the following theorem is derived.

Theorem 6 *Any simplicial deformation operation in each of the 6- and 18-neighborhood systems is described by a composition of a finite number of simplicial deformation operations by tetrahedral 3-simplexes in the 26-neighborhood system.*

Simplicial deformation operations by tetrahedral 3-simplexes are simply called elementary deformation operations.

7.4 Topology Preservation and Deformation

According to Theorems 5 and 6, any deformation operation is described as a composition of several elementary deformation operations. We then show that the topology is preserved by elementary deformation operations which are listed as DT1, DT2 and DT3 in Fig. 11. Let **V**, **E** and **F** be the numbers of the 0-,

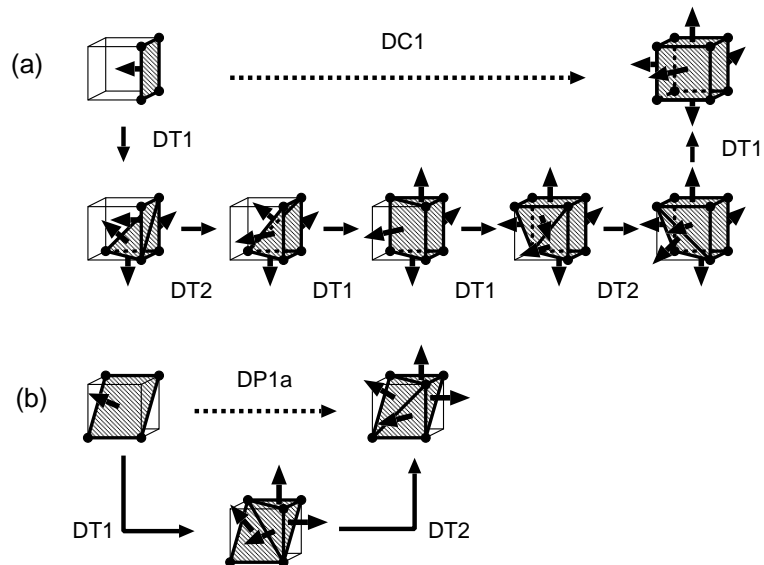


Fig. 12. Two examples of deformation operation decomposition. (a) A deformation operation by a cubic 3-simplex is decomposed into a series of six operations by tetrahedral 3-simplexes. (b) An operation by a pentahedral 3-simplex is decomposed into a series of two operations by tetrahedral 3-simplexes.

1- and 2-simplexes belonging to **Old**, respectively, and \mathbf{V}' , \mathbf{E}' and \mathbf{F}' be those belonging to **New**, respectively. In Table 2, these values for each of DT1, DT2 and DT3 are given. As the table shows, the following relation is derived for each operation:

$$(\mathbf{V}' - \mathbf{V}) - (\mathbf{E}' - \mathbf{E}) + (\mathbf{F}' - \mathbf{F}) = 0.$$

Clearly, this is equivalent to (4). In the case of shrinking, we can similarly show the topology preservation by replacing **Old** and **New** by **New** and **Old**, respectively, in Table 2.

Operation type	Old			New		
	V	E	F	V'	E'	F'
DT1	3	3	1	4	6	3
DT2	4	5	2	4	5	2
DT3	4	6	3	3	3	1

Table 2. The numbers of discrete simplexes of 0, 1 and 2 dimensions belonging to **Old** and **New** for each elementary operation for expanding deformation.

Let us consider any change of local topological properties of each point caused by a deformation operation. Table 3 shows all changes of local topological properties with respect to each elementary operation for expanding. For shrinking deformation, all changes are obtained if we replace **Old** and **New** by **New** and **Old**, respectively, in Table 3.

Operation type	Old	→	New
DT1	exterior point of the closed surface	→	cyclic point
	cyclic point	→	cyclic point
DT2	cyclic point	→	cyclic point
DT3	cyclic point	→	spherical point
	cyclic point	→	cyclic point

Table 3. All changes of local topological properties caused by each elementary operation for expanding deformation.

7.5 Deformation Algorithm

Assume that \mathbf{A} and \mathbf{B} are two discrete objects and $\partial\mathbf{A}$ and $\partial\mathbf{B}$ be their boundaries such that

$$E(\partial\mathbf{A}) = E(\partial\mathbf{B}) .$$

Note that both $\partial\mathbf{A}$ and $\partial\mathbf{B}$ are sets of finite numbers of discrete closed surfaces according to Theorem 2. We then consider the deformation from $\partial\mathbf{A}$ to $\partial\mathbf{B}$. In this subsection, $\partial\mathbf{A}$ and $\partial\mathbf{B}$ are expressed by polyhedral representations which we obtain using Algorithm 2. In addition, let $\mathbf{V}(\mathbf{A})$ and $\mathbf{V}(\mathbf{B})$ be sets of lattice points included in \mathbf{A} and \mathbf{B} , respectively. Then, for the sake of simplicity of our deformation algorithm, we assume

$$\mathbf{V}(\mathbf{A}) \subseteq \mathbf{V}(\mathbf{B}) .$$

We first focus on an algorithm for the expanding deformation from $\partial\mathbf{A}$ to $\partial\mathbf{B}$ with respect to the 26-neighborhood system.

Algorithm 3

input: *The boundaries of two discrete objects, $\partial\mathbf{A}$ and $\partial\mathbf{B}$.*

output: *A series of n discrete object boundaries which are generated in the deformation process for expanding from $\partial\mathbf{A}$ to $\partial\mathbf{B}$: $\partial\mathbf{A}_0(= \partial\mathbf{A})$, $\partial\mathbf{A}_1$, $\partial\mathbf{A}_2$, ..., $\partial\mathbf{A}_n(= \partial\mathbf{B})$.*

begin

1. *Set $\mathbf{V}(\mathbf{A})$ and $\mathbf{V}(\mathbf{B})$ to be the sets of all lattice points in $\partial\mathbf{A}$ and $\partial\mathbf{B}$ respectively;*

2. set $i := 0$; $\partial\mathbf{A}_i := \partial\mathbf{A}$; $\mathbf{V}(\mathbf{A}_i) := \mathbf{V}(\mathbf{A})$;
 3. **while** $\mathbf{V}(\mathbf{B}) \setminus \mathbf{V}(\mathbf{A}_i) \neq \emptyset$ **do**
 - 3.1 select a point $\mathbf{x} \in \mathbf{V}(\mathbf{B}) \setminus \mathbf{V}(\mathbf{A}_i)$ such that $\mathbf{N}_{26}(\mathbf{x}) \cap \partial\mathbf{A}_i \neq \emptyset$ and every $\mathbf{y} \in \mathbf{N}_{26}(\mathbf{x}) \cap \partial\mathbf{A}_i$ is cyclic with respect to $\partial\mathbf{A}_i$;
 - 3.2 consider eight different unit cubes $\mathbf{D}_j(\mathbf{x})$ for $j = 1, 2, \dots, 8$ all of which include \mathbf{x} ;
 - 3.3 set **OLD** to be a set of all discrete polyhedra included in $\partial\mathbf{A}_i$ in the region of $\cup_{j=1}^8 \mathbf{D}_j(\mathbf{x})$;
 - 3.4 regard \mathbf{x} and all points in $\mathbf{V}(\mathbf{A}_i)$ as 1-points, look up all discrete polyhedra in Table 1 for each $\mathbf{D}_j(\mathbf{x})$ where $j = 1, 2, \dots, 8$ and set **NEW** as a set of all of those discrete polyhedra;
 - 3.5 if every \mathbf{y} in **NEW** is cyclic with respect to $(\partial\mathbf{A}_i \setminus \mathbf{OLD}) \cup \mathbf{NEW}$, set $\partial\mathbf{A}_{i+1} := (\partial\mathbf{A}_i \setminus \mathbf{OLD}) \cup \mathbf{NEW}$, $\mathbf{V}(\mathbf{A}_{i+1}) := \mathbf{V}(\mathbf{A}_i) \cup \{\mathbf{x}\}$ and $i := i + 1$.
- end**

For the preservation of the topology of $\partial\mathbf{A}_i$, in step 3.1 the selection of \mathbf{x} such that every $\mathbf{y} \in \mathbf{N}_{26}(\mathbf{x}) \cap \partial\mathbf{A}_i$ is cyclic with respect to $\partial\mathbf{A}_i$ is important since this condition enables us to avoid the deformation at the singular points of $\partial\mathbf{A}_i$. Furthermore, the last step 3.5 also enables us to avoid the appearance of new singular points in $\partial\mathbf{A}_{i+1}$ and thus preserves the topology. In other words, if we cannot find \mathbf{x} in step 3.1 or if \mathbf{y} is not cyclic in step 3.5, it is impossible to obtain $\partial\mathbf{B}$ from $\partial\mathbf{A}$ following Algorithm 3.

In steps 3.3 and 3.4, **OLD** and **NEW** are determined as discrete surfaces in the union of eight unit cubes around \mathbf{x} , such as $\cup_{j=1}^8 \mathbf{D}_j(\mathbf{x})$. Since **NEW** which is a subset of $\partial\mathbf{A}_{i+1}$ is generated by referring the procedure of Table 1, it is derived from Theorem 4 that **NEW** is uniquely determined. An example of generating **NEW** from **OLD** around \mathbf{x} is illustrated in Fig. 13. In Fig. 13, we obtain four 3-polyhedra attached to **OLD**. These 3-polyhedra are considered to be the differences between **OLD** and **NEW**. Obviously, at most one 3-polyhedron is determined in each $\mathbf{D}_j(\mathbf{x})$, $j = 1, 2, \dots, 8$, for the deformation from $\partial\mathbf{A}_i$ to $\partial\mathbf{A}_{i+1}$.

With the same notation as Algorithm 3, we now explain more precisely how to obtain $\partial\mathbf{A}_{i+1}$ from $\partial\mathbf{A}_i$ in the example in Fig. 13. According to Theorem 5, any polyhedral deformation operation can be decomposed into several simplicial deformation operations. In Fig. 13, the set of four attached 3-polyhedra is decomposed into six 3-simplexes. If there exist $k(i)$ 3-simplexes which are attached to **OLD** and generate **NEW**, we can determine the boundaries of $k(i)$ discrete objects generated by the deformation from $\partial\mathbf{A}_i$ to $\partial\mathbf{A}_{i+1}$ as a sequence such as

$$\partial\mathbf{A}_{i(0)} (= \partial\mathbf{A}_i), \partial\mathbf{A}_{i(1)}, \partial\mathbf{A}_{i(2)}, \dots, \partial\mathbf{A}_{i(k(i))} (= \partial\mathbf{A}_{i+1}).$$

In this sequence $\partial\mathbf{A}_{i(l+1)}$ is obtained by one elementary operation from $\partial\mathbf{A}_{i(l)}$, and hence the topology is preserved. Therefore, the total number of all discrete

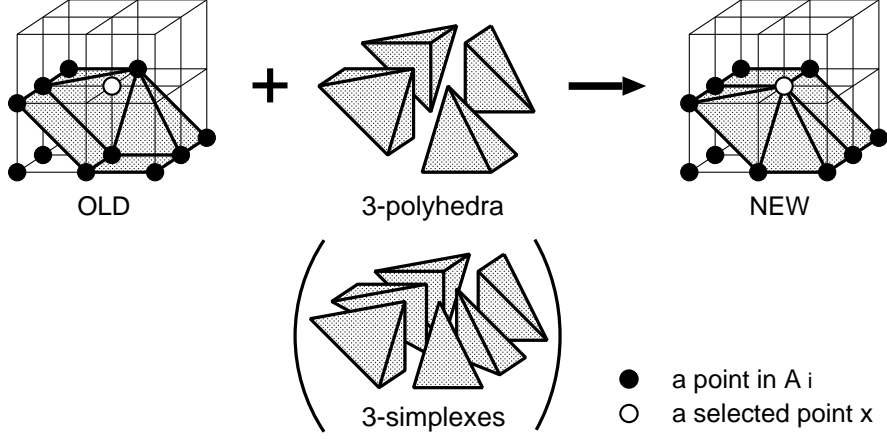


Fig. 13. An example of **OLD** and **NEW** generated around a selected point x in Algorithm 3. Four 3-polyhedra are attached to **OLD** for generating **NEW**. The simplicial decomposition of those four 3-polyhedra are also depicted.

object boundaries is $\sum_{i=1}^n k(i)$ in our deformation process from $\partial\mathbf{A}$ to $\partial\mathbf{B}$ which is described as

$$\partial\mathbf{A}_{0(0)} (= \partial\mathbf{A}), \partial\mathbf{A}_{0(1)}, \dots, \partial\mathbf{A}_{0(k(0))}, \partial\mathbf{A}_{1(1)}, \dots, \partial\mathbf{A}_{n(k(n))} (= \partial\mathbf{B}). \quad (8)$$

In this paper, we call (8) to be an expanding regular chain from $\partial\mathbf{A}$ to $\partial\mathbf{B}$; “regular” means that the topology is preserved. It is easy to check that the number of all possible expanding regular chains from $\partial\mathbf{A}$ to $\partial\mathbf{B}$ is finite. The value $\sum_{i=1}^n k(i)$ is called the length of the expanding regular chain (8); by notation, we denote the length of an expanding regular chain Γ by $L(\Gamma)$.

Now, let Γ be any expanding regular chain described by (8). Then its inverse

$$\partial\mathbf{A}_{n(k(n))} (= \partial\mathbf{B}), \dots, \partial\mathbf{A}_{n(k(1))}, \partial\mathbf{A}_{(n-1)(k(n-1))}, \dots, \partial\mathbf{A}_{0(k(0))} (= \partial\mathbf{A}), \quad (9)$$

is considered as a shrinking process from $\partial\mathbf{B}$ to $\partial\mathbf{A}$ by the deformation operations. We denote the process (9) by $\tilde{\Gamma}$, and call it a shrinking regular chain from $\partial\mathbf{B}$ to $\partial\mathbf{A}$. By definition, a regular chain is a composition of a finite number of expanding or shrinking regular chains.

For any pair of $\partial\mathbf{A}$ and $\partial\mathbf{B}$ so that there is at least one regular chain between them, we introduce the “deformation number” in the following way.

Definition 16 Given $\partial\mathbf{A}$ and $\partial\mathbf{B}$, we define the deformation number $d(\partial\mathbf{A}, \partial\mathbf{B})$ such that

$$d(\partial\mathbf{A}, \partial\mathbf{B}) = \min L(\Gamma),$$

where the minimum is taken over all regular chains from $\partial\mathbf{A}$ to $\partial\mathbf{B}$; if there is not regular chain from $\partial\mathbf{A}$ to $\partial\mathbf{B}$, we define $d(\partial\mathbf{A}, \partial\mathbf{B}) = +\infty$.

From the above definition, we can easily prove the following theorem.

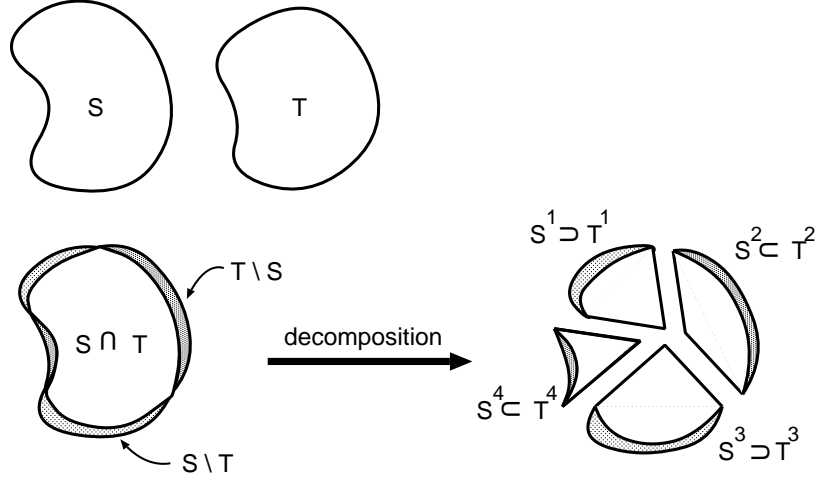


Fig. 14. An example of \mathbf{S} and \mathbf{T} so that $\mathbf{S} \cap \mathbf{T} \neq \emptyset$. The separation of \mathbf{S} and \mathbf{T} for calculation of $d(\partial\mathbf{S}, \partial\mathbf{T})$ is illustrated.

Theorem 7 *The following properties hold true:*

1. $d(\partial\mathbf{A}, \partial\mathbf{B}) \geq 0$;
2. $d(\partial\mathbf{A}, \partial\mathbf{B}) = 0$ if $\partial\mathbf{A} = \partial\mathbf{B}$;
3. $d(\partial\mathbf{A}, \partial\mathbf{B}) = d(\partial\mathbf{B}, \partial\mathbf{A})$;
4. $d(\partial\mathbf{A}, \partial\mathbf{B}) + d(\partial\mathbf{B}, \partial\mathbf{C}) \geq d(\partial\mathbf{A}, \partial\mathbf{C})$.

Fixing a discrete object \mathbf{P}_0 , we consider the space \mathbf{Y} which consists of all discrete objects \mathbf{P} such that there is a regular chain from $\partial\mathbf{P}_0$ from $\partial\mathbf{P}$. If we restrict $d(\cdot, \cdot)$ on $\mathbf{Y} \times \mathbf{Y}$, it gives a metric on \mathbf{Y} .

In order to compute $d(\partial\mathbf{S}, \partial\mathbf{T})$ for any pair of $\partial\mathbf{S}$ and $\partial\mathbf{T}$, we use Algorithm 3; Algorithm 3 gives the procedure for expanding $\partial\mathbf{A}$ to $\partial\mathbf{B}$ or shrinking $\partial\mathbf{B}$ to $\partial\mathbf{A}$ if $\mathbf{V}(\mathbf{A}) \subseteq \mathbf{V}(\mathbf{B})$. Therefore, it is necessary to decompose \mathbf{S} and \mathbf{T} into $\mathbf{S}^1, \mathbf{S}^2, \dots, \mathbf{S}^p$ and $\mathbf{T}^1, \mathbf{T}^2, \dots, \mathbf{T}^p$, respectively, such that

$$\mathbf{S}^i \subseteq \mathbf{T}^i \text{ or } \mathbf{T}^i \subseteq \mathbf{S}^i$$

for $i = 1, 2, \dots, p$. For each pair of $\partial\mathbf{S}_i$ and $\partial\mathbf{T}_i$, $i = 1, 2, \dots, p$, we can calculate $d(\partial\mathbf{S}_i, \partial\mathbf{T}_i)$ since the number of all possible regular chains Γ from $\partial\mathbf{S}_i$ to $\partial\mathbf{T}_i$ is finite. In many cases, it is not difficult to find such decompositions $\mathbf{S}^i, \mathbf{T}^i$ $i = 1, 2, \dots, p$, that

$$d(\partial\mathbf{S}, \partial\mathbf{T}) = \sum_{i=1}^p d(\partial\mathbf{S}^i, \partial\mathbf{T}^i).$$

See an example in Fig. 14.

In the 6- and 18-neighborhood systems, we can use Algorithm 3. Let \mathbf{A}_m and \mathbf{B}_m be two discrete objects in the m -neighborhood system for $m = 6, 18, 26$,

so that $\partial\mathbf{A}$ and $\partial\mathbf{B}$ are obtained from sets of lattice points, $\mathbf{V}(\mathbf{A})$ and $\mathbf{V}(\mathbf{B})$, respectively, by using Algorithm 2. Then, according to Theorem 3, the following relations are satisfied:

$$\bigcup_{[a] \in \mathbf{A}_6} |a| \subseteq \bigcup_{[a] \in \mathbf{A}_{18}} |a| \subseteq \bigcup_{[a] \in \mathbf{A}_{26}} |a|,$$

$$\bigcup_{[a] \in \mathbf{B}_6} |a| \subseteq \bigcup_{[a] \in \mathbf{B}_{18}} |a| \subseteq \bigcup_{[a] \in \mathbf{B}_{26}} |a|.$$

Clearly, a deformation process from $\partial\mathbf{A}_{26}$ to $\partial\mathbf{B}_{26}$ is obtained by employing Algorithm 3. Since Table 1 shows that the difference between $\partial\mathbf{A}_{26}$ and $\partial\mathbf{A}_{18}$ (resp. $\partial\mathbf{B}_{26}$ and $\partial\mathbf{B}_{18}$) is a set of tetrahedral 3-simplexes, a deformation from $\partial\mathbf{A}_{26}$ to $\partial\mathbf{A}_{18}$ (resp. from $\partial\mathbf{B}_{26}$ to $\partial\mathbf{B}_{18}$) is considered to be a shrinking process removing those 3-simplexes. Similarly, corresponding to $\partial\mathbf{A}_{26}$ and $\partial\mathbf{A}_6$ (resp. $\partial\mathbf{B}_{26}$ and $\partial\mathbf{B}_6$), a deformation from $\partial\mathbf{A}_{26}$ to $\partial\mathbf{A}_6$ (resp. from $\partial\mathbf{B}_{26}$ to $\partial\mathbf{B}_6$) is also considered to be a shrinking process removing tetrahedral 3-simplexes.

8 Conclusions

We introduced polyhedral representations of 3-dimensional objects and the closed surfaces in \mathbf{Z}^3 by using the combinatorial topology. We also established a method for constructing uniquely a set of closed surfaces from a given finite subset of \mathbf{Z}^3 . Our representation of discrete closed surfaces contains not only connectivity between neighboring points but the 2-dimensional topological structures as well. Using these topological structures, we can derive a deformation of discrete closed surfaces while preserving their topology with their dimensions. We first presented a finite set of all elementary deformation operations which are deformation operations by tetrahedral 3-simplexes as shown in Fig. 11. We then demonstrated that in any neighborhood system any other deformation operation can be represented by a composition of those elementary deformation operations. Furthermore, we gave an algorithm for the deformation between the boundaries of two discrete objects. Our algorithm enables us to calculate the number of elementary operations which are employed in a deformation process. We call this number the deformation number. Obviously, the deformation numbers give a metric for the similarity between any pair of two discrete objects which have equivalent topology.

References

1. J. O. Lachaud, A. Montanvert: Volumic Segmentation Using Hierarchical Representation and Triangulated Surface. Research Report **95-37** Laboratoire de l'Informatique du Parallélisme, Ecole Normale Supérieure de Lyon (1995)
2. T. Y. Kong, A. Rosenfeld: Digital Topology: Introduction and Survey. *Computer Vision, Graphics, and Image Processing* **48** (1989) 357–393

3. P. P. Jonker, O. Vermeij: On Skeletonization in 4D Images. *Advances in Structural and Syntactical Pattern Recognition, Proceedings of 6th International Workshop, SSPR'96*, Edited by P. Perner, P. Wang, A. Rosenfeld LNCS 1121 Springer-Verlag (1996) 79–89
4. K. Abe, F. Mizutani, C. Wang: Thinning of Gray-Scale Images with Combined Sequential and Parallel Conditions for Pixel Removal. *Visual Form Analysis and Recognition*, Edited by C. Arcelli, L. P. Cordella, G. S. Baja Plenum Press, New York (1991) 1–10
5. M. P. P. Schlicher, E. Bouts, P. W. Verbeek: Fast Analytical Medial-Axis Localization in Convex Polyhedra. *IEEE Proceedings of 13th International Conference on Pattern Recognition* (1996) 55–61
6. K. Voss: *Discrete Images, Objects, and Functions in \mathbf{Z}^n* . Algorithms and Combinatorics 11 Springer-Verlag, Berlin, Heidelberg (1993)
7. G. T. Herman: Discrete Multidimensional Jordan Surfaces. *CVGIP: Graphical Models and Image Processing* 54 (1992) 507–515
8. J. K. Udupa: Multidimensional Digital Boundaries. *CVGIP: Graphical Models and Image Processing* 56 (1994) 311–323
9. W. E. Lorensen, H. E. Cline: Marching Cubes: A High-Resolution 3D Surface Construction Algorithm. *Computer Graphics (SIGGRAPH '87)* 21 (1987) 163–169
10. J. Françon: Discrete Combinatorial Surface. *Graphical Models and Image Processing* 57 (1995) 20–26
11. P. S. Aleksandrov: *Combinatorial Topology I*. Graylock Press, Rochester, N.Y. (1956)
12. Y. Kenmochi, A. Imiya, A. Ichikawa: Discrete Combinatorial Geometry. *Pattern Recognition* (to appear)
13. Y. Kenmochi, A. Imiya, A. Ichikawa: Boundary Extraction of Discrete Objects. *Computer Vision and Image Understanding* (to appear)
14. Y. Kenmochi, A. Imiya: Deformation of Discrete Object Surfaces. *Computer Analysis of Images and Patterns, Proceedings of the 7th International Conference CAIP'97*, Edited by G. Sommer, K. Daniilidis, J. Pauli LNCS 1296 Springer-Verlag (1997) 146–153
15. A. Imiya, U. Eckhardt: Euler Characteristic of Discrete Objects. *Discrete Geometry for Computer Imagery 1997* LNCS Springer-Verlag (to appear)